21st International Symposium on
Mathematical Theory of Networks and Systems
July 7-11, 2014. Groningen, The Netherlands

A refined adaptive model reduction approach for control of fast evolving distributed parameter systems

Davood Babaei Pourkargar and Antonios Armaou[†]

Abstract— **The problem of output feedback control for fast evolving distributed parameter systems is investigated using adaptive proper orthogonal decomposition (APOD). The novelty lies in employing a modified data ensemble construction approach for APOD to construct models with enlarged region of accuracy. Modifying the construction procedure of ensemble snapshots in APOD allows the derivation of local valid low-dimensional reduced order dynamic models (ROMs) with enlarged region of accuracy for controller synthesis thus resulting in a computationally-efficient alternative to using large-dimensional models with global validity. This advantage is utilized for the synthesis of a robust state controller combined with a dynamic observer of the system states with an enlarged region of attraction. The proposed approach is successfully used to stabilize the Kuramoto-Sivashinksy equation at a spatially invariant steady state profile in the absence and presence of uncertainty when the open loop process exhibits highly nonlinear behavior. The original and the modified ensemble construction approaches for APOD are compared in different conditions and the effectiveness of the modified approach is presented.**

I. Introduction

In the past 30 years research has focused on the development of control structures for transport-reaction processes. Such distributed systems can be mathematically described by parabolic partial differential equations (PDEs). The control problem for these processes is nontrivial due to the spatially distributed nature of the associated system dynamics. A well established approach to address the control problem is via model reduction using weighted residual methods [8], [9], [11], [15]. For industrial processes of current interest the issue of complex spatial dynamics and domain limits the applicability of analytical model reduction methods. Statistical techniques circumvent this limitation via off-line construction of the required basis functions [1], [2], [12], [22], [23], [26].

A common approach to compute the reduced order model (ROM) is via a combination of a variant of proper orthogonal decomposition (POD) [23] with the method of weighted residuals to construct an ordinary differential equation (ODE) system. The original POD algorithm requires a priori availability of a sufficiently large ensemble of PDE solution data, called snapshots, to compute empirical basis functions. However, in practice, it is difficult to predict how to generate enough snapshots so that all possible dominant spatial modes are appreciably contained in the ensemble. The resulting basis functions, therefore, are representative of the corresponding ensemble only. During closed-loop simulation, situations can arise when the existing basis functions fail to accurately represent the dynamics of the PDE system.

One solution is to continue sampling on-line, enlarging the ensemble of snapshots, and then to recompute the basis functions. However, this would require the solution of the eigenvalue problem every time, which may become computationally expensive, and hence, unsuitable for on-line computations as the process evolves. To (a) achieve the computational load reduction and (b) circumvent the issue of a priori availability of a sufficiently large ensemble of PDE solution data, a recursive computation of basis functions, algorithm called adaptive proper orthogonal decomposition (APOD) can be used on-line [5], [22]. APOD is based on algebraic manipulations leading to a three-fold increase in computational speed compared to brute-force streaming methods and similar optimization based techniques allowing for its on-line implementation. In [4], [6], the requirements on continuous measurement sensors were then reduced using APOD-based dynamic observers. In [7], a criterion is derived to minimize the communication bandwidth from the distributed sensors to the APOD-based control structure using networked control concepts.

In this paper, another limitation of streaming method is addressed. Output feedback controllers are designed for fast evolving distributed parameter systems based on continuous point measurements available from limited number of sensors. The developed methodology for output feedback control is based on the successful integration of dynamic observers with static controllers. A refined ensembling approach is thought and used in APOD to recursively update the basis functions as the closed-loop process evolves through different regions of the state space based on maximizing retained information that is received from the distributed sensors. The proposed controllers are illustrated on the Kuramoto-Sivashinksy equation with and without uncertainty in the presence of highly nonlinear dynamics and chaotic behavior, where they are called to stabilize the system at an open-loop unstable system steady state.

II. Mathematical Preliminaries

We focus on the problem of stabilization using feedback control of spatially distributed processes described by the

Financial support from the National Science Foundation, CMMI Award # 13-00322 is gratefully acknowledged.

[†]Department of Chemical Engineering, The Pennsylvania State University, University Park, PA 16802, USA, Tel: +1(814) 865-5316, Fax: +1(814) 865-7846, Email addresses: dzb158@engr.psu.edu (D. Babaei Pourkargar; Student Member, IEEE, AIChE & SIAM), armaou@engr.psu.edu (A. Armaou; Corresponding Author, Senior Member, IEEE & AIChE)

ISBN: 978-90-367-6321-9

following description of highly dissipative PDEs

$$\begin{aligned}\frac{\partial}{\partial t}\bar{x}(z,t) &= \mathcal{A}(z)\bar{x}(z,t) + \mathcal{F}(z,\bar{x}) + b(z)u(t),\\ y_m(t) &= \int_\Omega s(z)\bar{x}(z,t)\,dz,\\ y_r(z,k) &= \int_0^t \delta(t-t_k)\bar{x}(z,t)\,dt,\end{aligned} \tag{1}$$

subject to the following boundary conditions

$$q(\bar{x}, \frac{\partial \bar{x}}{\partial z}, ..., \frac{\partial^{n_0-1}\bar{x}}{\partial z^{n_0-1}}) = 0 \text{ on } \partial\Omega, \tag{2}$$

and initial condition

$$x(z,0) = x_0(z). \tag{3}$$

In the above PDE system, t is the time, $z \in \Omega \subset \Re^3$ is the spatial coordinate and $x(z,t) \in \Re^n$ denotes the vector of state variables. $u = [u_1, u_2, ..., u_l] \in \Re^l$ denotes the vector of manipulated inputs. Ω is the domain of the process and $\partial\Omega$ is its boundary. $\mathcal{A}(z)$ and $\mathcal{F}(z,\bar{x})$ are linear and bounded Lipschitz nonlinear parts of spatial differential operator of order n_0, respectively. $b(z) \in \Re^{n\times l}$ is a known smooth matrix function of z of the form $[b_1(z)\ b_2(z)\ ...\ b_l(z)]$, where $b_i(z)$ describes how the i^{th} control action $u_i(t)$ is distributed in the spatial domain Ω; e.g. point actuation could be defined using standard Dirac delta. In (2), $q(\cdot)$ is a sufficiently smooth nonlinear vector function, $\frac{\partial^i \bar{x}}{\partial z^i}|_{\partial\Omega}$ for $i = 1, \ldots, n_0 - 1$, denotes the spatial derivatives in the direction perpendicular to the boundary and $\bar{x}_0(z)$ is a smooth vector function of z. The availability of two sets of measurement sensors is assumed: periodic distributed snapshot measurements, $y_r(z,k) \in \mathbb{R}^n$, and continuous measurements, $y_m \in \mathbb{R}^r$, where r is the number of continuous sensors and k is a discrete variable that indicates the sample time counter to taking the snapshots. Note that y_r indicates measured spatial profiles while y_m is a vector variable. $s(z)$ is the sensor shape functions corresponding to y_m and t_k is the time instance for snapshot measurement. In this manuscript, the results are presented for $\bar{x} \in \mathbb{R}$, however, it is straightforward to extend them for $\bar{x} \in \mathbb{R}^n$, by treating each state independently [23].

The control objective is to stabilize the process of (1)-(3) at a desired spatial profile, $x_d(z,t)$. Without loss of generality, we assume the spatially uniform steady state $x_d(z,t) = 0$ as the desired profile. The inner product and norm in the space of square integrable functions, $L_2[\Omega]$, is defined as

$$(\vartheta_1, \vartheta_2) = \int_\Omega \vartheta_1^T(z)\vartheta_2(z)dz \qquad \text{and} \qquad \|\vartheta_1\|_2 = (\vartheta_1, \vartheta_1)^{1/2}$$

where ϑ^T denotes the transpose.

III. Adaptive model reduction

A. Off-line and on-line computation of empirical basis functions

Similar to other data-driven pattern analysis methodologies, the state profiles of the system (snapshots) during process evolution are collected to construct the initial ensemble. This ensemble can be obtained either experimentally by initially gathering open-loop process evolution data before activating the controller or from previously obtained process history data, or by performing off-line numerical simulations of the PDE system. Let $v \in L_2^K$, $v_k = y_r(z,k)$ represents the snapshot in vector form where $y(z,k) = \bar{x}(z,t_k)$ denotes the snapshot of the system state available at time t_k. The off-line part of APOD is used to identify an orthogonal set of empirical basis functions that capture the dominant spatial patterns in the ensemble. It also provides a measure of the relative contribution of each basis function to the total energy of the ensemble. This is achieved using the covariance matrix of the ensemble, $C_K := (v^T, v^T)$, whose elements show the correlation between the snapshots. Then the solution of a computationally expensive eigenvalue problem of the spatial differential operator is thus replaced by the solution of an eigenvalue problem of the covariance matrix of the snapshot ensemble. This may also be computationally demanding depending on the ensemble size.

The key features of the off-line part of the algorithm and a detailed analysis have been presented in [5], [22]. Briefly, it is assumed that m eigenmodes capture ε of energy in the ensemble, i.e. $\sum_{i=1}^m \lambda_i / \sum_{i=1}^K \lambda_i \geq \varepsilon$, where the eigenvalues are ordered in terms of size as follows $\lambda_1 > \lambda_2 > \cdots > \lambda_K$. An orthonormal basis for the subspace $\mathbb{P}$ is obtained as:

$$\begin{aligned}Z &= [\omega_1\ \omega_2\ \cdots\ \omega_r],\ Z \in \mathbb{R}^{K\times m}\\ \Lambda &= [\lambda_i \Delta_{ij}]_{ij},\ i,j = 1, \ldots, m\end{aligned} \tag{4}$$

where ω_i denotes the i^{th} eigenvector of C_K that corresponds to the i^{th} eigenvalue, λ_i, and Δ_{ij} is the Kronecker delta. Note that the basis functions computed by these eigenvectors also capture the dominant dynamics of the PDE system of (1-3) locally. We can compute the vector of basis functions $\Psi = [\psi_1\ \psi_2\ \cdots\ \psi_m]^T$ as a linear combination of the snapshots given by the following equation

$$\Psi = \Lambda^{-1/2} Z^T v. \tag{5}$$

The eigenspace of the covariance matrix is thus partitioned into the dominant subspace contains the basis functions which capture at least ε of energy in the ensemble (denoted as $\mathbb{P}$) and the orthogonal complement to $\mathbb{P}$, which contains the rest of the modes (denoted as $\mathbb{Q}$). Such a partition is possible based on Assumption 1. Based on [22], the orthogonal projection operators P and Q onto subspaces $\mathbb{P}$ and $\mathbb{Q}$ can be computed as

$$P = ZZ^T,\ Q = I - ZZ^T \tag{6}$$

where I denotes the identity matrix of dimension K. The objective is to obtain the new basis Z when new snapshots of the process become available.

During system evolution, the recursive algorithm allows updating the empirical basis functions on-line once new measurements from the process become available. It bypasses the computational demands at each time step when a new snapshot is obtained. The orthonormal basis for subspace $\mathbb{P}$ is recursively updated upon the arrival of new snapshots, possibly by increasing or decreasing the size of the basis if required and by maintaining the accuracy of basis by performing orthogonal power iteration, while the

orthonormal basis for $\mathbb{Q}$ can be computed from the fact that $\mathbb{Q}$ is the orthonormal complement of $\mathbb{Q}$. The mentioned recursive process is computationally efficient as long as the dimension of $\mathbb{P}$ is small (which partly depends on choosing an appropriate value for ε and the system characteristics).

A flow chart illustrating the APOD approach and the associated algebraic computations are presented in Fig. 3. Note that in the flow chart, ξ corresponds to the contribution of the dominant eigenvalue of $c_q = QC_KQ$, namely λ_{m+1}, towards the total energy of the ensemble, i.e. $\xi = \lambda_{m+1}/\sum_{i=1}^{m+1}\lambda_i$, and $H = Z^TC_KZ$ is an $m \times m$ matrix (see [5], [22] for additional details).

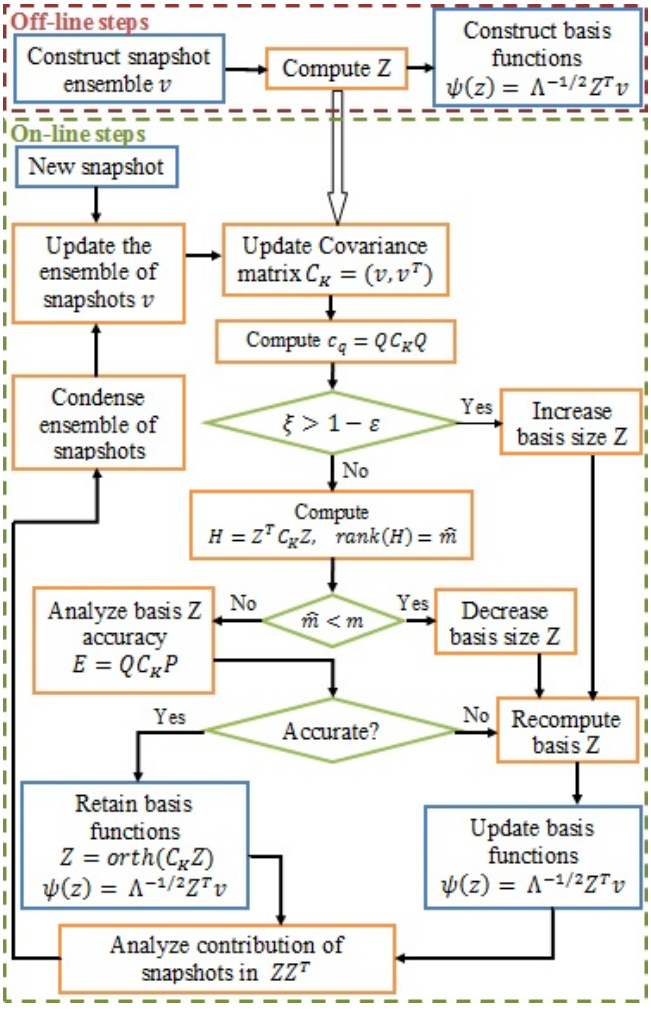

Fig. 1. Flow chart of APOD. Blue boxes denote algorithm I/Os and green boxes decision steps. APOD modifications involve changes to the procedure of ensemble update.

B. Ensemble update sequence

As new information is obtained during closed-loop process evolution by the periodic snapshot measurements, y_r, the following two approaches are considered to generate the new ensemble of snapshots that is used to compute the covariance matrix in the next time step when the new snapshot arrives,

1) The newest snapshots approach: In this approach the newest snapshots are considered in the ensemble of snapshots. In each time step during closed-loop process evolution the oldest snapshot of the system will be replaced by the new snapshot arrived by the periodic snapshot measurements, y_r. Thus, in each time step the ensemble only includes the most recent snapshots. In this paper APOD using this data ensembling is called the "original APOD".

2) The most important snapshots approach: The modification analyzes the contribution of snapshots in P by normalized dominant eigenvectors and search for the one which had the minimum L_2 norm per row and eliminate the corresponding snapshot in the ensemble. The mentioned snapshot could be eliminated before or after addition of the new snapshot since it is possible to eliminate the new data if the elimination takes place after augmenting the new snapshot. Thus the least important snapshots are eliminated before adding the new one, in order to have the most recent snapshot and also the most important ones. This is called the "modified APOD".

To formulate the procedure, consider the contribution column vectors of $D = \{d_j\}$ and standardization column vector of $S = \{s_j\}$, respectively, as follows

$$d_j = (P_AP_A^T)_{jj} \tag{7}$$

where $(\cdot)_{jj}$ indicates the diagonal element of $(\cdot)$ and

$$s_j = \|C_{K,j}\|_2, \tag{8}$$

where $\|\cdot\|_2$ indicates the 2-norm of vector $(\cdot)$ and $C_{K,j}$ means the j^{th} row of the covariance matrix and $j = 1,\ldots,K$.

The normalized snapshot contribution column vector, $N = \{n_j\}$, is defined based on (9)

$$n_j = \frac{d_j}{s_j}, \qquad j = 1,\ldots,K. \tag{9}$$

We eliminate the snapshot that corresponds to the element in the normalized snapshot contribution vector that has the lowest value.

In the original APOD, the ensemble of the snapshots that is used to update the basis functions only possesses the most recent snapshots. The procedure could possibly lead to loss of previously important profiles as the process evolves away from them and they are replaced by profiles that contain new information. If the process revisits a previously accessed state space region, APOD has to recapture the new trends as they reaffirm themselves leading to a lag in the ROM revision to capture the new trends. A move to consider the most important snapshots instead of newest ones thus leads to faster revision of the ROM when regions of the state space are previously revisited. Robust control design based on this ROM leads to larger region of accuracy which is important when dealing with model uncertainty and fast evolving processes.

C. Finite dimensional approximation using method of weighted residuals

Using the basis functions, the finite dimensional approximation of the infinite dimensional PDE system of (1)-(3) can be constructed based on the method of weighted residuals. $\bar{x}(z,t)$ can be generally described as an infinite weighted sum of a complete vectorized set of basis functions $\Psi(z)$.

$$\bar{x}(z,t) \simeq \sum_{k=1}^{m} \psi_k(z) a_k(t) \tag{10}$$

where $a_k(t)$ are time varying coefficients known as system modes. The following m^{th} order system of ODEs is obtained by substituting (10) in (1)-(3), multiplying the PDE with the weighting functions, $\varphi(z)$, and integrating over the entire spatial domain:

$$\begin{aligned} \sum_{k=1}^{m} (\varphi_v(z), \psi_k(z)) \dot{a}_k(t) &= \sum_{k=1}^{m} (\varphi_v(z), \mathcal{A}(z)\psi_k(z)) a_k(t) \\ &+ \big(\varphi_v(z), \mathcal{F}(z, \sum_{k=1}^{m} \psi_k(z) a_k(t))\big) + (\varphi_v(z), b(z))u, \\ v &= 1, ..., m, \\ y_m &= \sum_{k=1}^{m} (s(z), \psi_k(z)) a_k(t). \end{aligned} \tag{11}$$

The type of weighted residual method could be determined by the weighting functions in the above equation. The method of weighted residuals reduces to Galerkin's method when the weighting functions, $\varphi(z)$, and the basis functions, $\Psi(z)$, are the same. Then (11) can be summarized as

$$\begin{aligned} \dot{a} &= Aa + f(a) + Bu \\ y_m &= Ca \end{aligned} \tag{12}$$

where A, B and C are constant matrices and f is a nonlinear smooth vector function of the modes that can be described based on the comparison between (11) and (12). From Lipschitz condition of $\mathcal{F}$, we obtain that f satisfies local Lipschitz condition as follows

$$\Big\| f(a_1) - f(a_2) \Big\| \leq K_l \|a_1 - a_2\| \tag{13}$$

where K_l indicates the upper bound gain in the Lipschitz inequality.

Remark 1: The modified data ensembling approach increases the computation time of APOD by 10% however it leads to more robust ROMs that require revisions more infrequently.

Remark 2: In the proposed approach for model reduction the snapshots used are obtained during closed-loop system evolution as opposed to all other proper orthogonal decomposition-based reduction approaches that are based on open-loop snapshots, and thus, these snapshots and the resulting ROM account for the impact of controller functional form on the process. It is important to note this intimate relation between APOD and the controller.

D. Dynamic observer

We assume that the snapshots of the process become available only periodically and the point measurements from a restricted number of sensors are continuously available which is quite common in industrial processes. In [22], [26], static output observers based on the continuous point measurements were designed to estimate the modes of (11) that are required for controller design. The number of sensors must be supernumerary to the number of modes to successful estimate the modes of (11) using the linear static observers. This implies that numerous measurement sensors are required, otherwise the static observer gives unstable estimates. To overcome these issues, we employed a dynamic observer that conceptually needs only one point measurement to predict the dynamic behavior of the modes.

The theory on linear dynamic observer design was developed by Luenberger in [21] and offered a complete and comprehensive analysis. Nonlinear dynamic observer design is much more complicated and has received considerable attention in the last 30 years [18], [19], [25].

The resulting dynamic observer based on (12) will have the following structure

$$\dot{\hat{a}} = A\hat{a} + f(\hat{a}) + Bu + L(C\hat{a} - y_m) \tag{14}$$

where $\hat{a}$ is the vector of estimated modes, L is the observer gain and C is the output matrix.

Assuming observability and controllability [3], [14] of the system (12), we used pole placement approaches to compute the observer gain, L, that stabilizes the system of (14) in the Lyapunov sense. To implement the pole placement technique the observer error is defined as $e = \hat{a} - a$. The observer error dynamics can be defined using (12) and (14) as follows

$$\dot{e} = (A + LC)e + [f(\hat{a}) - f(\hat{a} - e)]. \tag{15}$$

The following Lyapunov function is considered

$$V = V_o + V_c = \frac{1}{2} e^T e + \frac{\zeta}{2} a^T a, \tag{16}$$

where V_o and V_c denote the observation Lyapunov function (OLF) and control Lyapunov function (CLF), respectively, and the time derivative of the Lyapunov function is $\dot{V} = e^T \dot{e} + \zeta a^T \dot{a}$.

Considering the control objective, $a \to 0$ and the CLF of $V_c = \frac{\zeta}{2} a^T a$, a controller can be designed that forces the time derivative of the CLF, $a^T \dot{a}$, to be negative. Then we need only establish that

$$\begin{aligned} \dot{V}_o &= e^T \dot{e} \\ &= e^T (A + LC)e + e^T [f(\hat{a}) - f(\hat{a} - e)] < 0 \end{aligned} \tag{17}$$

If f satisfies the Lipschitz condition as follows

$$\|f(\hat{a}) - f(\hat{a} - e)\| \leqslant K\|e\|, \tag{18}$$

then

$$\begin{aligned} e^T [f(\hat{a}) - f(\hat{a} - e)] &\leqslant \|e^T\| \|f(\hat{a}) - f(\hat{a} - e)\| \\ &\leqslant \|e^T\| K\|e\| = K\|e\|^2 = K e^T e. \end{aligned} \tag{19}$$

The inequality (17) can be written as follows using (19)

$$e^T(A+LC)e+e^T(KI)e<0 \Rightarrow e^T(A+LC+KI)e<0$$
$$\Rightarrow A+LC+KI<0,$$

where I is the identity matrix with appropriate dimension.

The above inequality problem can be solved using pole placement for $A+KI+LC=A_o+LC$. The closed loop observer error poles are the eigenvalues of $A_c=A_o+LC$, which can be arbitrarily assigned by proper selection of the observer gain matrix, L. We assumed the observer dynamics to be faster than the controller dynamics for the separation principle to hold. The observer gain matrix, L, is chosen such that

$$|sI-(A_o+LC)|=p_{des}(s) \tag{20}$$

where I is the identity matrix and p_{des} is the characteristic polynomial of desired poles.

Remark 3: The pole placement technique is fast but it can be badly conditioned if unrealistic locations have been chosen for closed loop poles. Generally we should avoid placing multiple poles at the same location and it typically requires high gain when the open-loop poles are weakly observable which in turn sensitizes the entire closed-loop structure to perturbations [17].

E. Output feedback controller design

We now focus on synthesizing a control structure that achieves the objective of regulating the system of (14) to the origin. The first step in formulating the control problem is to find a control Lyapunov function (CLF) which in this formulation would be

$$V_c=\frac{\zeta}{2}a^Ta. \tag{21}$$

The following control law is formulated based on [16], [24]

$$u_i(t)=-k(a,c_o)L_{B_i}V_c, \tag{22}$$

$$k(a,c_o)=\begin{pmatrix} c_o+\frac{L_{\mathcal{F}}V_c+\sqrt{(L_{\mathcal{F}}V_c)^2+(L_{B_i}V_c)^4}}{(L_{B_i}V_c)^2+\eta}, & L_{B_i}V_c\neq 0 \\ c_o, & L_{B_i}V_c=0 \end{pmatrix}$$

where $L_{\mathcal{F}}V_c=\frac{\partial V_c}{\partial a}\mathcal{F}$ and $L_{B_i}V_c=\frac{\partial V_c}{\partial a}B_i$ denote Lie derivatives. B_i indicates the i^{th} element of B corresponding to i^{th} manipulated variable and $F(a)=Aa+f(a)$. The time-derivative of Lyapunov function V_c along the trajectories of the closed loop system is

$$\dot{V}_c\leq -c_o(L_{B_i}V_c)^2-\sqrt{(L_{\mathcal{F}}V_c)^2+(L_{B_i}V_c)^4}. \tag{23}$$

Since $\dot{V}_c$ is negative definite, the controller in (22) stabilizes the parabolic PDE system of (1)-(3) provided that the ROM provides an accurate description of process dynamics. The proposed control structure has a number of tuning variables, some that are implicit (and are explicitly connected with the ROM) and others that are explicit, such as c_o, ζ and η.

By combining the model reduction procedure with the dynamic observer and controller synthesis methods, we obtain an output feedback controller structure that guarantees that the closed-loop system evolves to the desired steady state. In Figure 2 the closed-loop process is presented under the proposed control structure in a block diagram form. The specific controller structure recursively redesigns the observer/controller components whenever the reduced order model is revised to retain relevancy and enforce closed-loop stability.

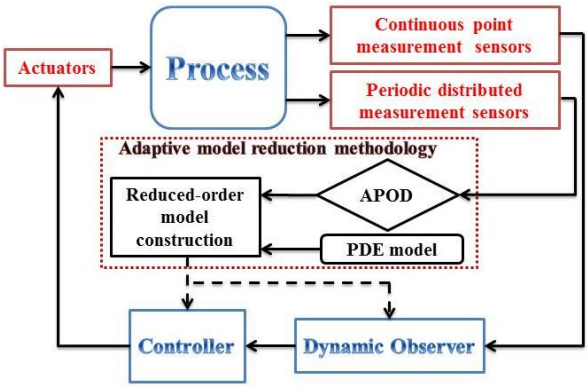

Fig. 2. Process operation block diagram under proposed controller structure.

Remark 4: The parameter c_o is used to shape the dynamic behavior of the closed-loop system. A large value of c_o makes $\dot{V}_c$ more negative and therefore generates a faster transient response. Note that a positive value of c_o is not necessary for stabilization.

Remark 5: When implementing the controller of (22), the control input near origin can exhibit chattering-like behavior due to round-off errors. This problem is circumvented by adding a sufficiently small positive number η to the $(L_{B_i}V_c)^2$ in the denominator of (22). The addition of this parameter obviously leads to some offset in the closed-loop response. However, this offset can be made arbitrarily small by choosing a sufficiently small value for η. A tradeoff thus exists between the smoothness of the control action (corresponds to large η) and the smaller offset in the closed-loop response (corresponds to using small value for η).

Remark 6: The Lyapunov function may periodically increase possibly due (a) to the well known observer peaking phenomenon and (b) during dimensionality changes of the ROM. The value of ζ needs be chosen appropriately to ensure that for the chosen controller parameters the Lyapunov functions during controller redesign satisfy the conditions of switched systems stability theorem [13]. We thus automatically adjust ζ at every instance of ROM change as follows

$$\zeta=\xi\frac{a^T(t_{k-1})\,a(t_{k-1})}{a^T(t_k)\,a(t_k)} \tag{24}$$

where t_k indicates the ROM revision instances during process operation. In general, higher values of ζ lead to more aggressive control action.

IV. Simulation Results

In this section, the ability of modified APOD in stabilizing the Kuramoto-Sivashinksy equation (KSE) is illustrated and compared to the original data ensembling approach in the

absence and presence of uncertainty. KSE can adequately describe incipient instabilities arising in a variety of physio-chemical systems including falling liquid films, unstable flame fronts, interfacial instabilities between two viscous fluids [10]. The dynamic behavior of KSE with periodic boundary conditions have revealed the existence of steady and periodic wave solutions, as well as chaotic behavior [20]. Feedback control of KSE has been well studied in the literature [12], [22]. The integral form of the controlled KSE

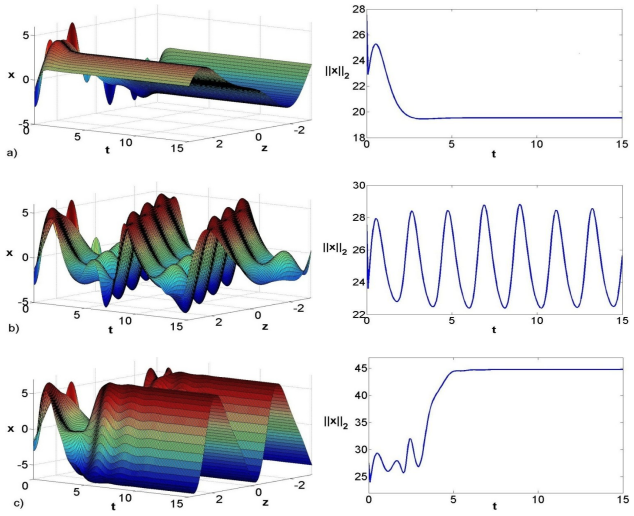

Fig. 3. Open-loop spatiotemporal state profile (left) and norm of the state (right) for (a) v = 0.4, (b) v = 0.23 and (c) v = 0.15.

that is considered is

$$\frac{\partial x}{\partial t} = -v\frac{\partial^4 x}{\partial z^4} - \frac{\partial^2 x}{\partial z^2} - x\frac{\partial x}{\partial z} + \sum_{i=1}^{l} b_i u_i(t) \qquad (25)$$

with periodic boundary conditions:

$$\frac{\partial^j x}{\partial z^j}(-\pi,t) = \frac{\partial^j x}{\partial z^j}(\pi,t), \qquad j = 0,...,3 \qquad (26)$$

and initial condition

$$x(z,0) = x_0(z), \qquad (27)$$

where $x(z,t)$ is the system variable, $u(t) \in \mathbb{R}^l$ is the vector of control variables, t is the time, z is the spatial coordinate, $b(z)$ is a row vector describing the control actuators and v is the diffusion parameter that can be a source of uncertainty in the KSE. Note that in (25) we have $\mathcal{A}(z) = -v\frac{\partial^4}{\partial z^4} - \frac{\partial^2}{\partial z^2}$ and $\mathcal{F}(x) = -x\frac{\partial x}{\partial z}$. The length of the spatial domain is 2π and six control actuators were assumed to be available at the following locations $L = [-\pi/2, -\pi/4, -\pi/6, \pi/5, \pi/4, \pi/2]$ and the corresponding spatial distribution functions at these locations are $b_i(z) = \delta(z - L_i)$ for $i = 1,...,6$. Note that the specific actuators affect all the modes of the system. Five continuous point measurement sensors placed uniformly across the domain of the process $(-\pi,\pi)$ are used. The continuous sensors shape distribution function, $s_m(z)$, at these respective positions is $s_{m,i}(z) = \delta(z - z_i)$ for $i = 1,...,5$, where z_i is the location of i^{th} sensor. The following spatially nonuniform initial condition was considered $x_0 = 3\sin(z) - \cos(2z) - \sin(5z) + 2\cos(5z)$. Figure 3 presents the open-loop profile and the spatial norm of the state of the KSE for $v = 0.4$, 0.23 and 0.15, respectively. We observe that KSE exhibits complex behavior for $v < 1$ and the profile $x = 0$ is open-loop unstable. Thus, the control objective is to stabilize the system of (25)-(27) at a desired spatial profile. Without loss of generality, we set the spatially uniform steady state $x_d(z,t) = 0$ as the desired profile.

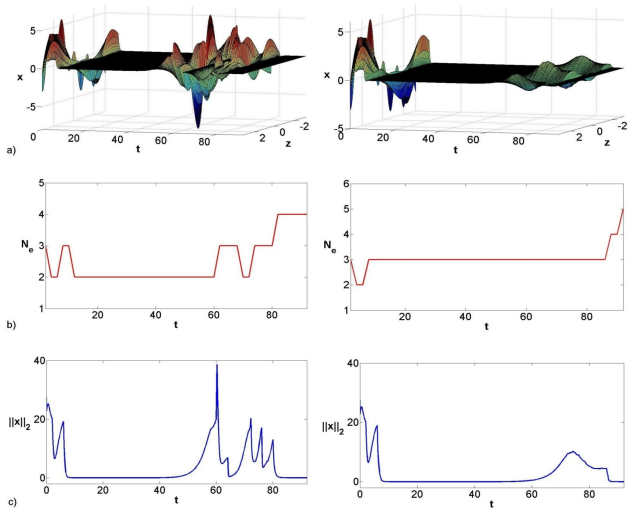

Fig. 4. Closed-loop temporal profiles of (a) the state spatial profile, (b) number of dominant basis functions and (c) norm of the state when v changes from 0.4 to 0.23 at $t = 40$. The left figures present results using original APOD and the right figures present results using modified APOD.

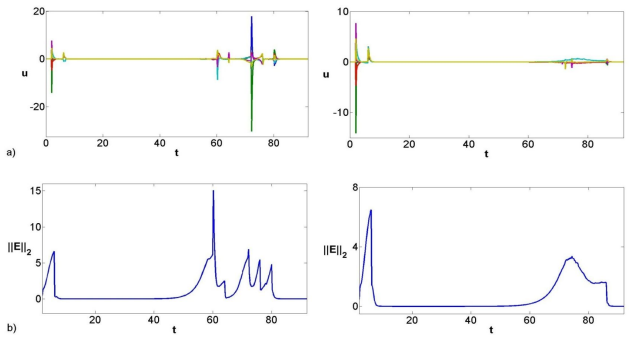

Fig. 5. Closed-loop temporal profiles of (a) control actions and (b) norm of error between the real system and the model when v changes from 0.4 to 0.23 at $t = 40$. The left figures present results when using original APOD and the right figures present results using modified APOD.

For both ensembling approaches, in order to obtain the initial basis functions we used 31 snapshots during the initial time period $t = [0,2]$; during this period the process evolves with $u(t) = 0$ (inactive controller). The following design parameter values were used to implement the control structure on the KSE: $\eta = 0.001$, $c_o = 0.8$, $\varepsilon = 0.99$ and $\zeta = 2$. Application of off-line APOD to this ensemble resulted in 3 basis functions for x which capture 99% of the energy embedded in the ensemble. As the availability of snapshots of the process is usually limited, we assume the availability of snapshots (complete profiles of the state) of the process every $t_s = 2$ units of time during closed loop operation whereas

point measurements from the five sensors are assumed to be available continuously. Figure 4 presents the closed-loop

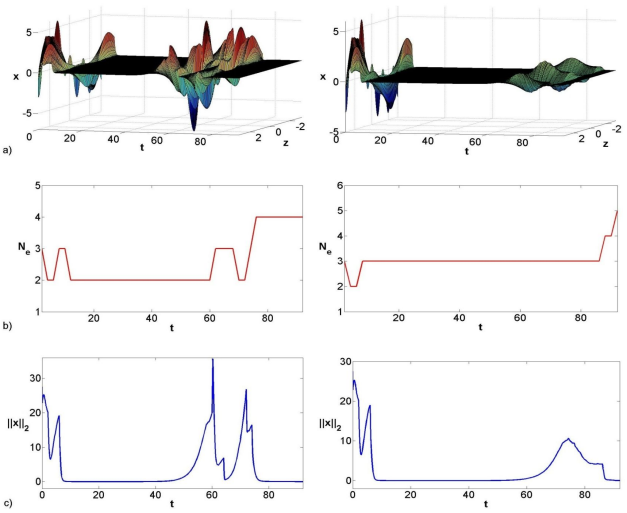

Fig. 6. Closed-loop temporal profiles of (a) the state spatial profile, (b) number of dominant basis functions and (c) norm of the state in the presence of uncertainty when v changes from 0.4 to 0.23 at $t = 40$. The left figures present results using original APOD and the right figures present results using modified APOD.

process profile, number of dominant basis functions and the norm of the state, respectively for the original and the modified APOD when the diffusivity parameter, v, changes from 0.4 to 0.23 at $t = 40$. The controller is informed of the change in this case, called "without any uncertainty". We observe that the controller successfully stabilizes the system of (25)-(27) at the $x(z,t) = 0$ while the L_2 norms converge smoothly to zero without any peaking for both approaches. In both cases the success of the designed controller in stabilizing the process at the desired profile is due to the dominant eigenspace (hence the ROM and the control law) being updated as the process traverses through different regions of the state space during closed-loop operation. The number of basis functions required to capture the initial trends was 3. During the closed-loop process operation, when new trends appeared the dominant eigenspace dimension was updated to accurately capture the process behavior, appropriately changing the number of empirical basis functions. We observe that even though the change in v takes place at 40, it take 10 seconds for the new trends to become appreciable and another 5 seconds for them to necessitate a dimensionality change for ROM in order to capture all the unstable eigenmodes.

Figure 5 shows the control actions and the norms of error between the real system and the ROMs. Using both approaches, the control actions and the model errors converge to zero and we do not observe any chattering when the parameter of the system changes and the controller/observer pairs is cognizant this change. To compare the performance of the two approaches, we defined two performance indices: INC, the integral of norm of the control actions and INE, the integral of norm of the error between the real system and the model. The smaller values of INC and INE, the

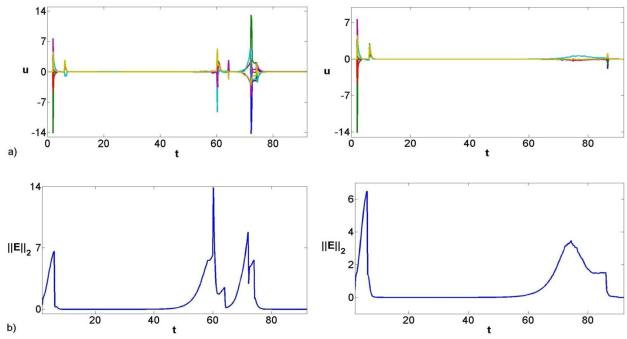

Fig. 7. Closed-loop temporal profiles of (a) control actions and (b) norm of error between the real system and the model in the presence of uncertainty when v changes from 0.4 to 0.23 at $t = 40$. The left figures present results using original APOD and the right figures present results using modified APOD.

less control effort and more accurate model, respectively. When v changes from 0.4 to 0.23 without any uncertainty the following indices shows the better performance of modified approach rather than the original approach in APOD, $INC_{or} = 93.02, INC_{mod} = 34.01, INE_{or} = 98.63, INE_{mod} = 62.01$ where "or" and "mod" indicate using the original and the modified ensembling approach in APOD. Based on the indices we conclude that the modified APOD generated a more accurate ROM and constructed a better controller in this case. In the presence of uncertainty when the con-

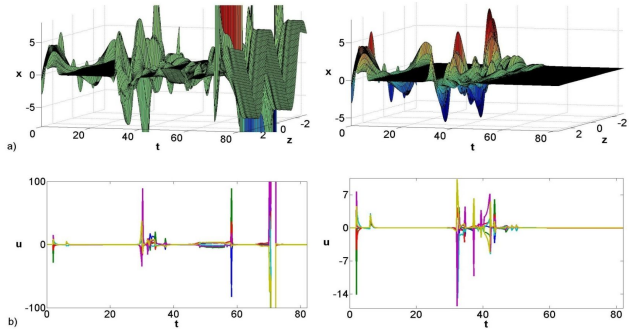

Fig. 8. Closed-loop temporal profiles of (a) the state spatial profile and (b) control actions in the presence of uncertainty when v changes from 0.4 to 0.15 at $t = 25$. The left figures present results when using original APOD and the right figures present results using modified APOD.

troller is not aware of the changes the effectiveness of the modified approach becomes more prominent. Figure 6 shows the closed-loop process profile, number of dominant basis functions and the norm of the state, respectively for the original and the modified APOD when the diffusivity parameter, v, changes from 0.4 to 0.23 at $t = 40$ when the controller and the dynamic observer are not informed about the parameter change. We observe that the controllers still successfully stabilize the system of (25)-(27) at $x(z,t) = 0$ while the L_2 norms converge smoothly to zero without any peaking. Figure 7 shows the control actions and the norms of error between the real system and the ROMs. Using both approaches, the control actions and the model errors converge to zero and we do not observer any chattering when the parameter of the system changes. The following indexes

indicate that the modified APOD has better performance compared to the original approach. $INC_{or} = 95.77$, $INC_{mod} = 32.66$, $INE_{or} = 90.73$, $INE_{mod} = 62.30$. Figure 8 presents the case when the diffusivity parameter, v, changes from 0.4 to 0.15 at $t = 25$ unbeknownst to the control structure. The original APOD not only could not regulate the process but also it destabilized the process while the refined approach still could stabilize the closed-loop process at the desired steady state profile using reasonable control action.

V. Conclusions

The output feedback control issue of fast evolving distributed parameter systems with limited state measurements was addressed. By combining a robust state controller with a dynamic observer of the system states and employing modified approach in APOD methodology, we synthesized computationally efficient control structures. The proposed approach was successfully used to regulate the Kuramoto-Sivashinksy equation at a spatially invariant steady state profile in the absence and presence of uncertainty when the open loop process exhibits highly nonlinear and chaotic behavior. The original and the modified ensemble construction approaches for APOD were compared under different conditions and the effectiveness of the modified approach was illustrated.

References

[1] A. Armaou and P. D. Christofides, *Nonlinear feedback control of parabolic PDE systems with time-dependent spatial domains*, J. Math. Anal. Appl., 239 (1999), pp. 124–157.

[2] A. Armaou and P. D. Christofides, *Plasma-enhanced chemical vapor deposition: Modeling and control*, Chem. Eng. Sci., 54 (1999), pp. 3305–3314.

[3] A. Armaou and M. A. Demetriou, *Optimal actuator/sensor placement for linear parabolic PDEs using spatial H_2 norm*, Chem. Eng. Sci., 61 (2006), pp. 7351–7367.

[4] D. Babaei Pourkargar and A. Armaou, *Control of dissipative partial differential equation systems using APOD based dynamic observer designs*, in Proceedings of the American Control Conference, Washington, DC, 2013, pp. 502–508.

[5] D. Babaei Pourkargar and A. Armaou, *Modification to adaptive model reduction for regulation of distributed parameter systems with fast transients*, AIChE J., 59(12) (2013), pp. 4595–4611.

[6] D. Babaei Pourkargar and A. Armaou, *Design of APOD-based switching dynamic observers and output feedback control for a class of nonlinear distributed parameter systems*, J. Proc. Cont., to appear (2014).

[7] D. Babaei Pourkargar and A. Armaou, *Feedback control of linear distributed parameter systems via adaptive model reduction in the presence of device network communication constraints*, in Proceedings of the American Control Conference, Portland, OR, 2014, to appear.

[8] M. J. Balas, *Feedback control of linear diffusion processes*, Int. J. Control, 29 (1979), pp. 523–533.

[9] M. J. Balas, *Nonlinear finite-dimensional control of a class of nonlinear distributed parameter systems using residual mode filters: A proof of local exponential stability*, J. Math. Anal. Appl., 162 (1991), pp. 63–70.

[10] H. C. Chang, *Nonlinear waves on liquid film surfaces i. flooding in vertical tube*, Chem. Eng. Sci., 41 (1986), pp. 2463–2476.

[11] P. D. Christofides, *Nonlinear and Robust Control of PDE Systems*, Birkhäuser, New York, 2000.

[12] P. D. Christofides and A. Armaou, *Global stabilization of the kuramoto-sivashinsky equation via distributed output feedback control*, Sys. & Contr. Lett., 39 (2000), pp. 283–294.

[13] P. D. Christofides and N. El-Farra, *Control of Nonlinear and Hybrid Process Systems: Designs for Uncertainty, Constraints and Time-Delays*, Springer-Verlag, Berlin, Germany, 2005.

[14] R. F. Curtain and H. Zwart, *An Introduction to Infinite-Dimensional Linear Systems Theory*, Springer-Verlag, New York, 1995.

[15] M. A. Demetriou and R. C. Smith, *Research directions in distributed parameter systems*, SIAM Frontiers in Applied Mathematics, Philadelphia, (2003).

[16] N. El-Farra and P. D. Christofides, *Robust inverse optimal control of nonlinear systems*, Int. J. Robust Nonlinear Control, 13 (2003), pp. 1371–1388.

[17] T. Kailath, *Linear systems*, Prentice-Hall, 1980.

[18] I. Karafyllis and C. Kravaris, *Robust output feedback stabilization and nonlinear observer design*, Sys. & Contr. Lett., 54 (2005), pp. 925–938.

[19] N. Kazantzis and C. Kravaris, *Nonlinear observer design using lyapunov's auxiliary theorem*, Sys. & Contr. Lett., 34 (1998), pp. 241–247.

[20] I. G. Kevrekidis, B. Nicolaenko, and J. C. Scovel, *Back in the saddle again: a computer assisted study of the kuramoto-sivashinsky equation*, SIAM J. Appl. Math., 50 (1990), pp. 760–790.

[21] D. G. Luenberger, *Observing the state of a linear system*, IEEE Trans. Milit. Electr., 8 (1963), pp. 74–80.

[22] S. Pitchaiah and A. Armaou, *Output feedback control of distributed parameter systems using adaptive proper orthogonal decomposition*, Ind. Eng. Chem. Res., 49 (2010), pp. 10496–10509.

[23] L. Sirovich, *Turbulence and the dynamics of coherent structures: part I, II and III*, Quarterly of Applied Mathematics, XLV (1987), pp. 561–590.

[24] E. Sontag, *A universal construction of artsteins theorem on nonlinear stabilization*, Sys. & Contr. Lett., 13 (1989), pp. 117–123.

[25] M. Soroush, *Nonlinear state-observer design with application to reactors*, Chem. Eng, Sci., 52 (1997), pp. 387–404.

[26] A. Varshney, S. Pitchaiah, and A. Armaou, *Feedback control of dissipative distributed parameter systems using adaptive model reduction*, AICHE J., 55 (2009), pp. 906–918.